Rapid sintering of inkjet printed Cu complex inks using Laser in air

Nihesh Mohan
Institute of Innovative Mobility (IIMo)
Technische Hochschule Ingolstadt
Ingolstadt, Germany
Nihesh.Mohan@thi.de

Juan Ignacio Ahuir-Torres
School of Engineering
Liverpool John Moores University
Liverpool, United Kingdom
J.I.AhuirTorres@ljmu.ac.uk

Sri Krishna Bhogaraju
Institute of Innovative Mobility (IIMo)
Technische Hochschule Ingolstadt
Ingolstadt, Germany
SriKrishna.Bhogaraju@thi.de

Hiren Kotadia
School of Engineering
Liverpool John Moores University
Liverpool, United Kingdom
H.R.Kotadia@ljmu.ac.uk

Gordon Elger
Institute of Innovative Mobility (IIMo)
Technische Hochschule Ingolstadt
Ingolstadt, Germany
Gordon.Elger@thi.de

***Abstract*—Cu complex inks offer a facile and cost-effective alternative to commercial nanoparticle inks for printed electronics application. Cu complex inks are prepared by mixing Cu formate tetrahydrate (metal precursor) with amino-2-propanol (complexing agent) in a molar ratio of 1:2. A carrier solvent consisting of ethanol and ethylene glycol is then added to help adjust the rheological properties of the ink for printing purpose. The Cu complex ink having a viscosity of 12 mPa.s is then inkjet printed onto a polyimide substrate (thickness: 125 µm). After printing 10 layers, the ink is pre-dried under air at 100°C for 5 minutes followed by sintering using an IR laser (942 nm) to enable rapid thermal decomposition of the Cu formate. After sintering using a 100 W line beam laser scanned at 3 mm/sec under air; a contiguous and homogenous Cu metallic trace is formed with a minimum bulk resistivity of 4.8 µΩcm (2.84 times of bulk Cu). The laser sintered trace exhibited a highly compact and homogenous sintered structure after thermal decomposition compared to the conventional oven sintering process. Th result is remarkable and proves the importance of faster decomposition process. In contrast, sintering the same trace using slow ramp rate within the traditional oven sintering pr process, it is observed that a Cu metallic trace is formed with particles in the range of 2-5 µm that are sparsely distributed due to low metal content of Cu complex inks (< 10 metal wt.%). Due to sparse distribution of particles, a low bulk resistivity value of 102 µΩcm is obtained.**

Keywords—Cu complex inks, Laser sintering, Flexible substrate, Printed electronics

I. INTRODUCTION

Printed electronics provides an innovative approach using principles of traditional printing process to fabricate electronic devices on flexible and unconventional substrates using functional materials [1-5]. These functional materials mainly consist of conductive inks that can be printed onto suitable substrates by utilizing various printing techniques. These printing techniques can be classified as contact (flexographic printing, screen printing and soft lithography) and non-contact (inkjet printing, aerosol jet printing and direct writing technologies) patterning processes [5-7]. Among these printing technologies, non-contact patterning process provides advantages in terms of flexibility in design, higher patterning accuracy and lower risk of contamination [5-7]. Using this emerging technology, industries have the potential to produce low-cost, lightweight, and flexible electronic devices with applications such as wearable sensors, RFID components, energy harvesting and storage, thin film transistors, health monitoring devices and many more [8-17].

Over the last decade, there has been rapid development and commercialization of conductive Ag, Cu and Au nanoparticles (NPs) inks for printed electronics applications [18-22]. Noble metals like Ag and Au offer high conductivity and stability in terms of oxidation, however owing to high cost they are not suitable for large volume applications. On the other hand, Cu offers a good alternative due to its high electrical conductivity (58 MS/m, second only to Ag), higher abundance (1000 times more than Ag) and low cost (nearly 100 times cheaper than Ag) [23]. The biggest challenge however is addressing it's high affinity to oxidation at elevated temperatures (formation of Cu_2O at 150°C) [24]. Cu NPs are prone to oxidation due to its high surface energy, which leads to formation of surface oxide layers that hinder the sintering [25]. To tackle this issue, the sintering process is required to be done under an inert (N_2) or reducing atmosphere (formic acid enriched nitrogen, H_2 or forming gas). Aside from this, capping agents (such as Polyvinylpyrrolidone) are used not only to prevent oxidation of Cu NPs at lower temperatures, but also to prevent them from agglomerating within the ink formulation [26-27]. This leads to a complex synthesis route of Cu NPs ink. And typically, higher sintering temperature (>250°C) remove these capping agents to provide good sinterability [28]. Other issues pertaining to Cu NP inks are storage (refrigeration or deep freeze) and shorter shelf life (< 6 months).

In recent years, there has been a growing interest in development of Cu particle free inks [29-30]. It offers a facile and low-cost synthesis route, where nanoparticles are generated *in-situ* upon thermal decomposition. These inks are usually composed of Cu metal salt (mainly Cu formate tetrahydrate) and an amine based solvent that coordinates with formate ion in a monodentate or bidentate fashion to form a metal salt-amine complex [31]. Further, suitable solvents are added to improve the properties (viscosity and wettability) of the ink related to printing purpose. Since, the Cu exists in an ionic form, it prevents oxidation, particle agglomeration and provides a longer shelf life at room temperature. Additionally, these inks have lower decomposition temperature (<160°C) making it suitable for sintering on some polymeric substrates.

Based on these advantages, it also provides flexibility in terms of choosing a wide range of sintering processes for fabrication of conductive traces. Conventional oven sintering of Cu

complex inks faces many challenges. It requires use of an inert/reducing atmosphere because the formed NPs due to their reactivity are prone to oxidation. Also, efficient degassing of organics is required for fabrication of contiguous conductive traces [32]. Therefore, slower ramp rate (typically 5°C/min) is required for controlled evaporation of solvents present in the ink which in turn lead to formation of larger aggregates ranging from 2-5 µm [32]. This leads to sparse distribution of metallic particles resulting in poor conductivity of the metallic traces. Apart from conventional sintering processes under inert/reducing atmosphere, there have been several studies carried out using laser sintering, photonic sintering, microwave sintering and electrical sintering processes [33-37]. Among them Laser sintering provides several advantages in terms of high speed localized sintering preventing substrate damage to low melting point substrates (such as PET) and integration of patterning and sintering process for large scale production [33-34].

In this work, a comparison is made between the conventional oven sintering process and laser sintering process. Laser sintering of Cu complex inks is performed under air on a flexible polyimide substrate using two different types of laser optics (spot laser and line beam laser). Focus is made on laser sintering of fine printed structure (trace thickness after sintering < 1-2 µm and trace width < 100 µm) using inkjet printer. The challenges related to process optimization of laser sinter parameters will also be briefly discussed.

II. Experimental

A. Material

Cu (II) formate tetrahydrate (Cuf), (98%) is purchased from Thermo Fischer Scientific. Amino-2-propanol (A2P) (93%) is purchased from Sigma-Aldrich. Ethanol (>96%), and Ethylene glycol (EG) (>99%) are purchased from Carl Roth. Polyimide films (Kapton® HPPST-125 µm) from DuPont are used for printing. Apart from Cu (II) formate tetrahydrate and polyimide film, other chemicals are used as received. Additionally, propylene glycol methyl ether acetate (PGMEA) is used for cleaning of the ink cartridges and isopropanol is used to clean the substrates.

B. Synthesis

A Cuf-A2P complex is prepared by mixing in a molar ratio of 1:2. The mixture is then stirred for 15 minutes at 500 rpm in a planetary-rotary solder paste mixer (Thinky SR500). Then, an ink formulation for inkjet printing is prepared using ethanol and EG (mixed together in 75:25 wt. ratio). 6 g of Cuf-A2P complex is added to 6 g of ethanol-EG solvent combination to prepare a low viscosity ink of 12 mPa.s, essential for ink-jet printing with a Cu metal content of 7wt.% Cu. The viscosity of the inks was measured using a viscometer (Thermo Scientific Haake TM Viscotester TM) and the contact angle of the inks formed on polyimide substrate were measured using a drop shape analyser (Kruss DSA 30M). After the ink synthesis, spectral absorbance of the Cu complex ink is measured under near infrared (NIR) until 1050 nm using a spectrometer (PMA-12 Photonic multichannel analyser from Hamamatsu) to check the compatibility of the laser for performing the sintering experiments.

C. Printing and processing

The prepared Cu complex ink is printed using a Dimatix Materials Printer (DMP-2850, Fujifilm Dimatix Inc.) onto the polyimide substrates. Before printing, the polyimide substrates were Ar-plasma treated for 5 minutes for activation of the surface and removing of contaminations. The Ar-plasma treatment is done using Zepto PLS from Diener electronic under UV in a manually controlled Ar atmosphere with chamber pressure maintained between 0.4-0.45 mbar. After printing, a conventional oven sintering, and laser sintering process is conducted. A two-step process, pre-drying and sintering is conducted in a reflow oven (UniTemp RSS 160-S) under a constant N_2 flow of 5L/min. The pre-drying is done at 100°C for 5 min followed by sintering at a slow ramp rate of 5°C/min upto 160°C and then to 250°C for an isothermal holding time of 5 min. A predrying step is also conducted before the laser sintering process at 100°C for 5 min in air. Laser sintering of printed Cu complex ink traces are done using a spot (200W T-SMILS, optic size: 1.6 mm in diameter, wavelength: 940 nm) and line beam (360 W T-SPOLD, optic size: 2mm x 80mm, wavelength: 940 nm) laser from Hamamatsu Photonics Deutschland GmbH.

D. Characterization

The particle morphology and sinterability of fabricated traces after sintering are analyzed and measured using an optical microscope(Keyence VHX-900F 3D microscope). They are evaluated using a scanning electron microscope (Verse FEI dual beam) with following parameters (Electron High Tension: 10 KV, Working Distance: 10 mm, Current: 8 nA, Mode: Secondary Electrons). The thickness (t) of the trace was measured using an optical light profilometer (Nanofocus µ-surf custom) and sheet resistance (R_s) measured using a 4-point probe (Keithley 2461). The bulk or volume resistivity (ρ), thereafter is calculated using the following equation [38]:

$$\rho = t * R_s \quad (1)$$

Additionally, the bulk resistivity (ρ) can also be calculated using a standard formula as shown in equation 2 [38]:

$$\rho = R * \frac{w.t}{L} \quad (1)$$

where, R is the measured resistance and L, w, t are length, width, and thickness of the sintered trace.

III. Results and Discussion

A. Ink design and printability

Cuf upon thermal decomposition (>200°C) forms following by-products as shown in equation 2 and 3 [39]:

$$Cu(HCOO)_{2(s)} + heat \rightarrow Cu_{(s)} + 2CO_{2(g)} + H_{2(g)} \quad (2)$$

$$Cu(HCOO)_{2(s)} + heat \rightarrow Cu_{(s)} + CO_{2(g)} + CO_{(g)} + H_2O_{(g)} \quad (3)$$

A Cuf-A2P complex is prepared which decreases the thermal decomposition temperature to 160°C. The A2P in the complex helps in stabilizing the ink formulation preventing agglomeration and increasing the shelf life. The OH^- bond in the alkanolamine also promotes solubility with low-boiling point alcohol-based solvents (such as ethanol) that may help in lowering the viscosity of prepared complex for inkjet printing purpose. In order to prepare the ink for printing purpose using inkjet printing, it must have a viscosity in the range of 10-12 mPa.s. A solvent combination is prepared

using ethanol and EG in 75:25 wt. ratio, which then added to the complex in a 50:50 wt.% resulting in a viscosity of 12 mPa.s. In the prepared ink, ethanol is responsible for controlling the viscosity of the ink. EG is responsible for providing good stability by decreasing the rate of evaporation during printing as well as storage and improving patterning onto polyimide substrate by increasing the contact angle from 10° to 45°. This prevents uneven spreading and formation of single droplets instead of contiguous trace. Fig. 1a shows a schematic of drop deposition based on ink-substrate interaction, where γ_T and γ_E are surface tension of the ink and surface energy of the substrate, respectively. When surface tension of the Cu complex ink is very less than the surface energy of the polyimide substrate, it causes uneven spreading whereas when it is greater it causes droplet formation on the substrate [40]. In this case, the surface tension of the designed Cu complex ink is 35 mN/m and surface energy of the polyimide substrate is 47 mJ/m^2 [41]. Fig. 1b shows the contact angle measurement of the Cu complex ink with and without the presence of EG on polyimide substrate. In addition, printing parameters related to inkjet printing also play a key role in determining the uniformity and resolution of the printed pattern. Printing parameters such as waveform design, jetting voltage and drop spacing plays a significant role in controlling the drop volume, drop velocity and accurate placement of each drop in concurrence with the print design, respectively. Fig. 2 shows the inkjet printing parameters used in this study. More details related to optimization of printing parameters related to inkjet printing can be found in our previous publications [40].

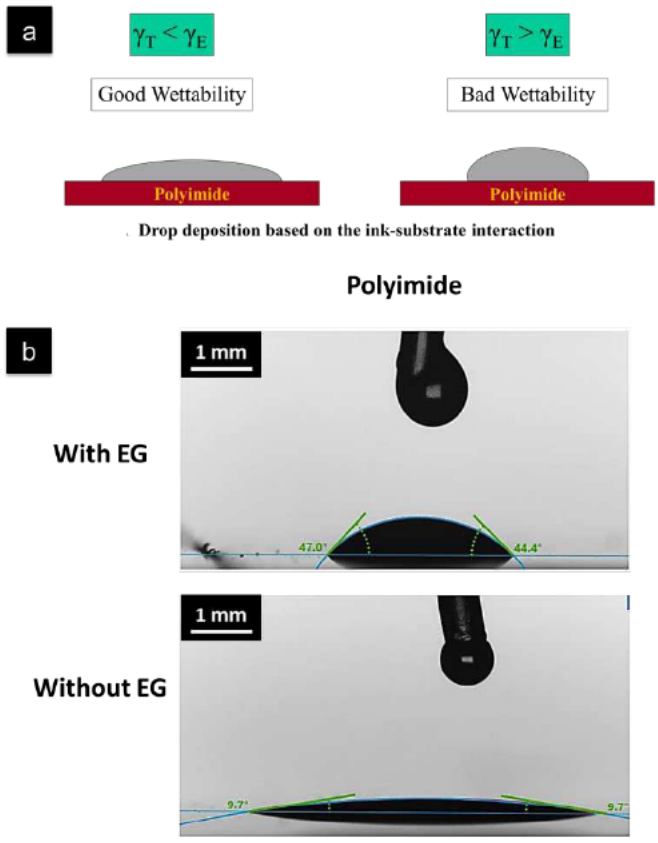

Fig. 1 Contact angle measurement of the Cu complex ink with and without the presence of EG on polyimide substrate.

a

Printing Parameters	Values/ Ranges
Printhead type	Samba™
Drop size (in volume, pL)	2.4
Number of nozzles in use	4-8
Jetting frequency (kHz)	50
Jetting voltage (V)	40
Cartridge temperature	Room temperature
Print head height (mm)	0.75
Drop spacing (µm)	15

b

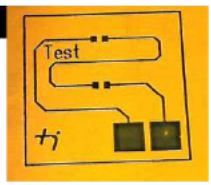

Fig. 2 Inkjet printing parameters for Cu complex ink and the design after printing.

B. Conventional oven sintering process

Firstly, the Cu complex ink traces after inkjet printing are subjected to conventional oven sintering. Cu complex inks have high volume shrinkage due to low solids content (<10 wt.% metallic Cu), therefore a slower ramp rate is necessary for efficient degassing of organics. The first step involves predrying of the printed Cu complex ink at 100°C for 5 mins followed by a slow ramp rate process upto 160°C at 5°C/min and then sintering at 250°C for 5 min. From the previous investigations, it was observed that using the slow ramp rate upto 160°C (decomposition temperature for A2P), a controlled evaporation of ink byproducts and better patterning post-sintering was achieved [32]. The *in-situ* realized NPs were then further sintered at 250°C for 5 mins. This method helped in fabricating contiguous traces, however showed a poor conductivity. Fig. 3a shows the differences in formation of Cu sintered trace when sintered using a slow ramp rate process and fast ramp rate process. Fig. 3b shows the SEM images of the Cu trace sintered using the slow ramp rate process (5°C/min). It was observed that large Cu aggregates (2-5 µm) were formed resulting in sparse distribution of particles across the sintered trace. The bulk resistivity of the Cu traces obtained was 102 µΩcm. It should be noted that unlike screen printing or other deposition methods, the thickness of printed trace is < 20 µm where the complex ink has a Cu metal content of < 7 wt.%. Aggregation of NPs is a tightly bound collection, where NPs are held together by strong mechanical forces that are difficult to breakup [42]. Usually as NPs form, they have high surface energy, and they tend to reduce this surface energy either by routes of agglomeration or aggregation [42]. This can however be thwarted via surface engineering (use of surfactants) or by use of rapid sintering methods (the nucleation and growth rate of NPs are increased with heating temperature and time) [42-43]. Therefore, rapid sintering processes using laser are required to produce a fine and homogenous sintered structure, where formed NPs are <100 nm and the resulting Cu metallic trace has high electrical conductivity.

C. Laser sintering process

In order to find a laser with suitable wavelength for laser sintering, the spectral absorbance of the Cu complex ink is measured. Fig. 4a shows the setup for measuring spectral absorbance using the spectrometer. It is observed that stronger transmission is observed in the blue region of visible spectrum with a peak value of 477.8 nm and stronger absorbance is observed in the red region of visible spectrum with a peak value of 700.64 nm. Fig. 4b shows the spectral absorbance of Cu complex ink. Based on this measurement, it is clear that a laser in the red or NIR spectrum should be selected for the laser sintering process. From the available

lasers, a laser of wavelength 940 nm was selected for the sintering process. Another important parameter to consider is selection of a suitable laser optic (spot laser and line beam laser).

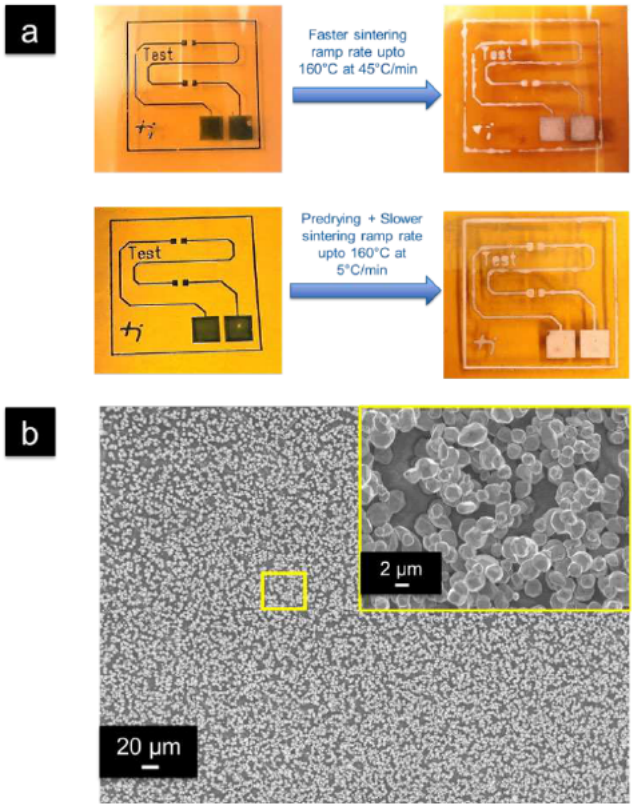

Fig. 3 (a) Inkjet printed pattern before and after sintering processes, faster ramp rate (top) and predrying plus slower ramp rate (bottom), (b) SEM image of the sintered sample after predrying followed by slower sintering ramp rate upto 160°C at 5°C/ min and then sintered at 250°C for 5 mins.

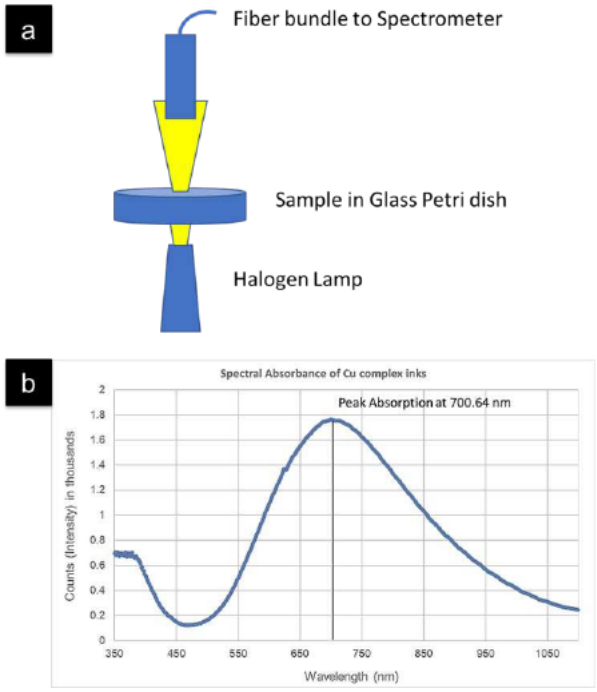

Fig. 4 (a) Setup for measuring spectral absorbance of Cu complex ink using the spectrometer, (b) Spectral absorbance of Cu complex ink.

After inkjet printing 10 layers of Cu complex ink, the printed traces are then predried at 100°C for 5 mins under air to avoid rapid evaporation of ethanol present in the ink. After process optimization, a spot laser of 1.6 mm diameter with a laser power of 10 W was used to sinter three identical printed traces using three different scan rates (30 mm/s, 20 mm/s and 10 mm/s). Using laser sintering parameters such as laser power (P), scan rate (v) and laser spot diameter (d) energy density (E_d) was calculated. Equation 4 shows the formula for calculation of energy density.

$$E_d = \frac{P}{v.d} \quad (4)$$

It was found that when scan rate was 30 mm/s, the calculated energy density was 20J/cm^2 which resulted in a partially sintered sample with large voiding as seen on the trace resulting in an inhomogeneous trace. Similarly, for a scan rate of 10 mm/s, the energy density was 62.5 J/cm^2 which caused substrate damage and subsequent oxidation of the trace. Using a scan rate of 20 mm/s, a sintered conductive trace having a sheet resistance of 3.2 Ω/□ under air was obtained, where energy density was calculated to be 31.25 J/cm^2. The trials with spot laser showed good sinterability between the Cu nanoparticles, however there was trace inhomogeneity and large voiding due to uneven heat distribution across the printed trace (see Fig. 5). From the experiments, the energy density is calculated to be in the range of 20-50 J/cm^2 for well sintered samples without causing substrate damage.

Subsequently, laser sintering was performed using a line beam laser with optic size of 2 mm x 80 mm. The operational advantages of using a line beam laser are larger scanning area which enables sintering of intricate designs without the need for retracing the printed path and its suitability for large scale production. They require however higher power to meet the required energy density for sintering the same printed trace resulting in higher operational costs. After process optimization, using a laser power of 100W and scanning rates of 12mm/s and 3mm/s sheet resistances of 1.2 Ω/□ and 0.8 Ω/□ were obtained respectively under air. Fig 5 shows the SEM images of laser sintered Cu complex traces using laser scan rate of 3mm/s. From SEM images, a well sintered homogenous structure is observed. The energy density calculated was found to be 30 J/cm^2, which aligns well with the good sinterability range as discussed earlier. Compared to spot laser, line beam laser provided an easy laser processing of the sintered traces without requiring any retracing of printed trace using g-codes. It also enabled complete sintering of printed traces without leaving behind any residual ink in the sintered traces. This can however be adjusted using a spot laser with larger spot diameter. Based on the profilometer results, the sintered trace formed using spot laser (for scan rate 20 mm/s) had an average thickness of 1.5 ± 0.8 µm, however the sintered trace formed using a line beam laser (for scan rate 3 mm/s) had an average thickness of 1.2 ± 0.2 µm. This resulted in a bulk resistivity (measured over a trace length of 20mm and average trace width of 1mm) of 24 µΩcm and 4.8 µΩcm for spot laser and line beam laser respectively. Using line beam laser, sintered Cu traces had bulk resistivity 2.84 times that of bulk Cu.

When compared with conventional oven sintering process, it is found that laser sintering in general produces a finer and densely packed structure. Further, in case of laser sintering the *in-situ* generated particles are exposed for a very short time (<100 ms) preventing the coalescence of the particles into larger aggregates [34]. In Fig. 5 (SEM images), it can be inferred that the particles formed tend to coalesce together in form of rod like structure in that short process time generating a densely packed web like structure [34]. Further it can be seen that after sintering using a line beam laser, this structure has a more uniform and packed structure. This can be attributed to the homogenous heat distribution. Further process optimization related to spot laser trials are ongoing, as it provides an advantage in terms of integration with the printing process and to understand the physical mechanism of laser sintering of Cu complex inks.

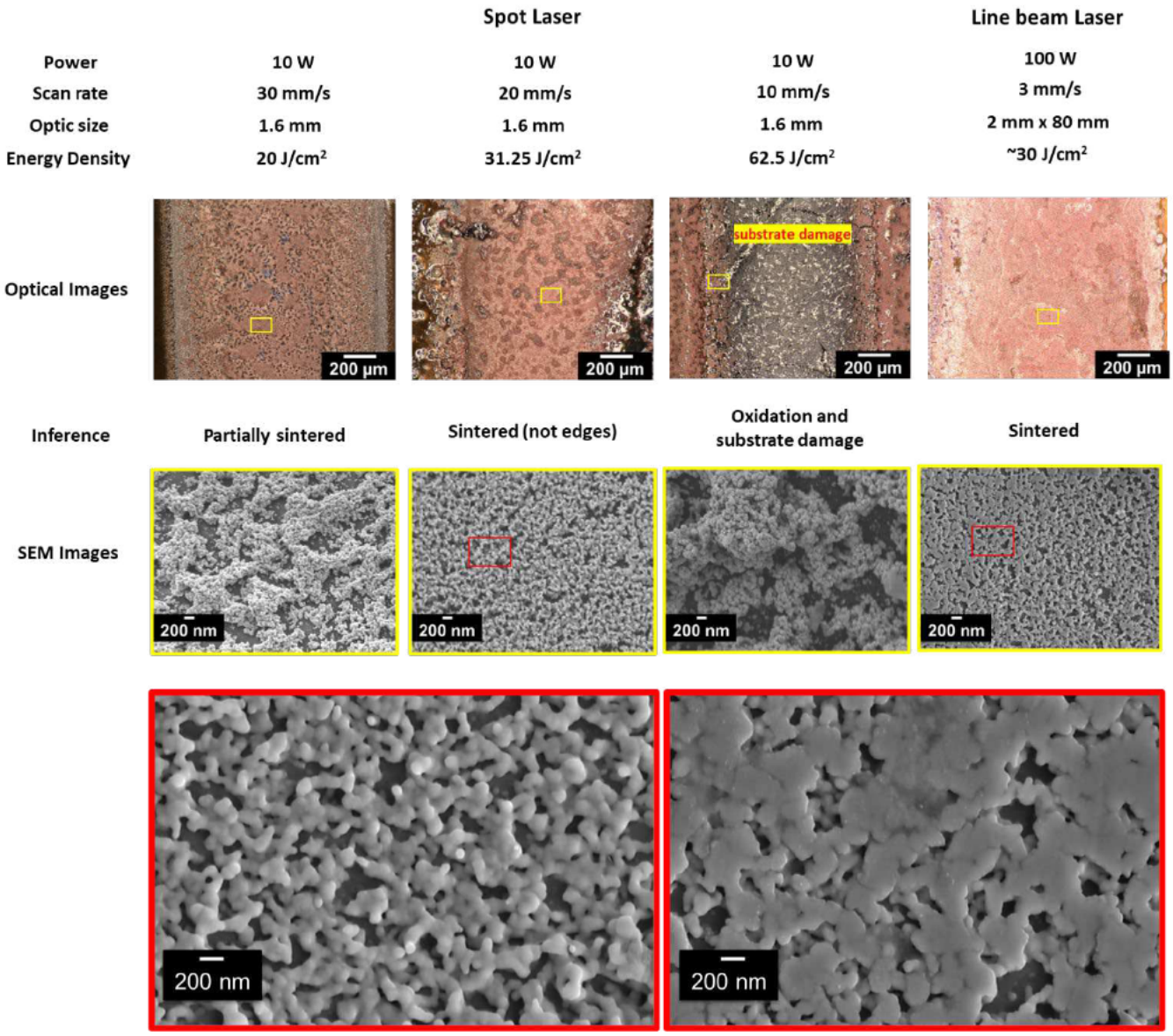

Fig. 5 Laser parameters, optical and SEM images of laser sintered sample using a spot laser of 1.6 mm diameter and line beam laser of optic size 2 mm x 80 mm.

IV. Conclusion

Cu complex inks provide a facile, low-cost alternative to nanoparticles-based inks for printed electronics application. Since, they exist in ionic form, they don't exhibit issues of agglomeration during storage and oxidation at ambient temperature. Using conventional reflow oven process, they can be sintered at temperature less than 160°C. However, post printing these inks require efficient degassing to prevent discontinuity of sintered traces post sintering process. Sintering using conventional process tend to form larger aggregates (2-5 µm) contributing to sparse distribution of particles within the sintered trace affecting the overall bulk resistivity (102 µΩcm). One method to solve this problem is using rapid sintering method such as laser sintering. Initial trials with spot laser showed good sinterability between the nanoparticles however trace inhomogeneity was an issue due to uneven heat distribution caused by the spot laser. Using

line beam optic laser, the morphology of the sintered trace was more homogeneous compared to the one obtained by spot laser as the scanning area is larger and helps in uniform heat distribution. The measured bulk resistivity was 24 μΩcm and 4.8 μΩcm for spot laser and line beam laser respectively. Using line beam laser, sintered Cu traces had bulk resistivity 2.84 times that of bulk Cu. In addition, the laser sintering was performed under air, and it also gives a possibility for sintering onto low melting temperature substrates such as PET.

V. Acknowledgment

The authors gratefully acknowledge the experimental support provided by external partners especially Hamamatsu Photonics Deutschland GmbH (Laser sintering) and Conti Temic microelectronic GmbH (Contact angle measurements). This research was funded by the German Ministry of Education and Science within the scope of project 'ADDIRA'.

References

[1] Khan, Y., Thielens, A., Muin, S., Ting, J., Baumbauer, C., & Arias, A. C. (2020). A new frontier of printed electronics: flexible hybrid electronics. Advanced Materials, 32(15), 1905279.

[2] Suganuma, K. (2014). Introduction to printed electronics (Vol. 74). Springer Science & Business Media.

[3] Kamyshny, A., & Magdassi, S. (2014). Conductive nanomaterials for printed electronics. Small, 10(17), 3515-3535.

[4] Cui, Z. (2016). Printed electronics: materials, technologies and applications. John Wiley & Sons.

[5] Beedasy, V., & Smith, P. J. (2020). Printed electronics as prepared by inkjet printing. Materials, 13(3), 704.

[6] Cruz, S. M. F., Rocha, L. A., & Viana, J. C. (2018). Printing technologies on flexible substrates for printed electronics. In Flexible electronics. Intech Open.

[7] Zhang, H., Moon, S. K., & Ngo, T. H. (2020). 3D printed electronics of non-contact ink writing techniques: status and promise. International Journal of Precision Engineering and Manufacturing-Green Technology, 7, 511-524.

[8] Sreenilayam, S. P., Ahad, I. U., Nicolosi, V., Garzon, V. A., & Brabazon, D. (2020). Advanced materials of printed wearables for physiological parameter monitoring. Materials Today, 32, 147-177.

[9] Kim, J., Kumar, R., Bandodkar, A. J., & Wang, J. (2017). Advanced materials for printed wearable electrochemical devices: A review. Advanced Electronic Materials, 3(1), 1600260.

[10] Kim, S. (2020). Inkjet-printed electronics on paper for RF identification (RFID) and sensing. Electronics, 9(10), 1636.

[11] Subramanian, V., Chang, P. C., Lee, J. B., Molesa, S. E., & Volkman, S. K. (2005). Printed organic transistors for ultra-low-cost RFID applications. IEEE transactions on components and packaging technologies, 28(4), 742-747.

[12] Subramanian, V., Fréchet, J. M., Chang, P. C., Huang, D. C., Lee, J. B., Molesa, S. E., ... & Volkman, S. K. (2005). Progress toward development of all-printed RFID tags: materials, processes, and devices. Proceedings of the IEEE, 93(7), 1330-1338.

[13] Grande, L., Chundi, V. T., Wei, D., Bower, C., Andrew, P., & Ryhänen, T. (2012). Graphene for energy harvesting/storage devices and printed electronics. Particuology, 10(1), 1-8.

[14] Kim, S., Tentzeris, M. M., & Georgiadis, A. (2019). Hybrid printed energy harvesting technology for self-sustainable autonomous sensor application. Sensors, 19(3), 728.

[15] Mirshojaeian Hosseini, M. J., & Nawrocki, R. A. (2021). A review of the progress of thin-film transistors and their technologies for flexible electronics. Micromachines, 12(6), 655.

[16] He, Y., Wang, X., Gao, Y., Hou, Y., & Wan, Q. (2018). Oxide-based thin film transistors for flexible electronics. Journal of Semiconductors, 39(1), 011005.

[17] Ma, L. Y., & Soin, N. (2022). Recent progress in printed physical sensing electronics for wearable health-monitoring devices: A review. IEEE Sensors Journal, 22(5), 3844-3859.

[18] Jung, I., Jo, Y. H., Kim, I., & Lee, H. M. (2012). A simple process for synthesis of Ag nanoparticles and sintering of conductive ink for use in printed electronics. Journal of electronic materials, 41, 115-121.

[19] Dang, M. C., Dang, T. M. D., & Fribourg-Blanc, E. (2014). Silver nanoparticles ink synthesis for conductive patterns fabrication using inkjet printing technology. Advances in Natural Sciences: Nanoscience and Nanotechnology, 6(1), 015003.

[20] Jeong, S., Song, H. C., Lee, W. W., Lee, S. S., Choi, Y., Son, W., ... & Ryu, B. H. (2011). Stable aqueous based Cu nanoparticle ink for printing well-defined highly conductive features on a plastic substrate. Langmuir, 27(6), 3144-3149.

[21] Dai, X., Xu, W., Zhang, T., & Wang, T. (2018). Self-reducible Cu nanoparticles for conductive inks. Industrial & Engineering Chemistry Research, 57(7), 2508-2516.

[22] Deng, M., Zhang, X., Zhang, Z., Xin, Z., & Song, Y. (2014). A gold nanoparticle ink suitable for the fabrication of electrochemical electrode by inkjet printing. Journal of nanoscience and nanotechnology, 14(7), 5114-5119.

[23] W. Li, Q. Sun, L. Li, J. Jiu, X.-Y. Liu und M. Kanehara, „The rise of conductive copper inks: challenges and perspective," Applied Materials Today, Bd. 18, Nr. 100451, 2019.

[24] Castrejón-Sánchez, V. H., Solís, A. C., López, R., Encarnación-Gomez, C., Morales, F. M., Vargas, O. S., ... & Sánchez, G. V. (2019). Thermal oxidation of copper over a broad temperature range: Towards the formation of cupric oxide (CuO). Materials Research Express, 6(7), 075909.

[25] Roy, N. K., Foong, C. S., & Cullinan, M. A. (2018). Effect of size, morphology, and synthesis method on the thermal and sintering properties of copper nanoparticles for use in microscale additive manufacturing processes. Additive Manufacturing, 21, 17-29.

[26] Li, W., Li, W., Wei, J., Tan, J., & Chen, M. (2014). Preparation of conductive Cu patterns by directly writing using nano-Cu ink. Materials Chemistry and Physics, 146(1-2), 82-87.

[27] Li, W., Chen, M., Wei, J., Li, W., & You, C. (2013). Synthesis and characterization of air-stable Cu nanoparticles for conductive pattern drawing directly on paper substrates. Journal of nanoparticle research, 15, 1-10.

[28] Deng, D., Jin, Y., Cheng, Y., Qi, T., & Xiao, F. (2013). Copper nanoparticles: aqueous phase synthesis and conductive films fabrication at low sintering temperature. ACS applied materials & interfaces, 5(9), 3839-3846.

[29] Shin, D. H., Woo, S., Yem, H., Cha, M., Cho, S., Kang, M., ... & Piao, Y. (2014). A self-reducible and alcohol-soluble copper-based metal–organic decomposition ink for printed electronics. ACS applied materials & interfaces, 6(5), 3312-3319.

[30] Yabuki, A., Tachibana, Y., & Fathona, I. W. (2014). Synthesis of copper conductive film by low-temperature thermal decomposition of copper–aminediol complexes under an air atmosphere. Materials Chemistry and Physics, 148(1-2), 299-304.

[31] Farraj, Y., Grouchko, M., & Magdassi, S. (2015). Self-reduction of a copper complex MOD ink for inkjet printing conductive patterns on plastics. Chemical Communications, 51(9), 1587-1590.

[32] Mohan, N., Saccon, R., Bhogaraju, S. K., & Elger, G. (2022, November). Cu complex inks for printed electronics application-challenges and solutions. In Mikro-Nano-Integration; 9. GMM-Workshop (pp. 1-5). VDE.

[33] Min, H., Lee, B., Jeong, S., & Lee, M. (2017). Fabrication of 10 μm-scale conductive Cu patterns by selective laser sintering of Cu complex ink. Optics & Laser Technology, 88, 128-133.

[34] Lee, J., Lee, B., Jeong, S., Kim, Y., & Lee, M. (2014). Microstructure and electrical property of laser-sintered Cu complex ink. Applied surface science, 307, 42-45.

[35] Araki, T., Sugahara, T., Jiu, J., Nagao, S., Nogi, M., Koga, H., ... & Suganuma, K. (2013). Cu salt ink formulation for printed electronics using photonic sintering. Langmuir, 29(35), 11192-11197.

[36] Kwon, Y. T., Kim, Y. S., Lee, Y., Kwon, S., Lim, M., Song, Y., ... & Yeo, W. H. (2018). Ultrahigh conductivity and superior interfacial adhesion of a nanostructured, photonic-sintered copper membrane for printed flexible hybrid electronics. ACS applied materials & interfaces, 10(50), 44071-44079.

[37] Zhang, J., Yuan, Y., Liang, G., Arshad, M. N., Albar, H. A., Sobahi, T. R., & Yu, S. H. (2015). A microwave-facilitated rapid synthesis of gold nanoclusters with tunable optical properties for sensing ions and fluorescent ink. Chemical Communications, 51(52), 10539-10542.

[38] Apostolakis, A., Barmpakos, D., Pilatis, A., Patsis, G., Pagonis, D. N., Belessi, V., & Kaltsas, G. (2022). Resistivity study of inkjet-printed structures and electrical interfacing on flexible substrates. Micro and Nano Engineering, 15, 100129.

[39] Bhogaraju, S. K., Mokhtari, O., Conti, F., & Elger, G. (2020). Die-attach bonding for high temperature applications using thermal decomposition of copper (II) formate with polyethylene glycol. Scripta Materialia, 182, 74-80.

[40] Mohan, N., Bhogaraju, S. K., Łysień, M., Schneider, L., Granek, F., Lux, K., & Elger, G. (2021, September). Drop feature optimization for fine trace inkjet printing. In 2021 23rd European Microelectronics and Packaging Conference & Exhibition (EMPC) (pp. 1-6). IEEE.

[41] Akram, M., Bhowmik, S., Jansen, K. M. B., & Ernst Leo, J. (2010). Surface modification of polyimide by atmospheric pressure plasma for adhesive bonding with titanium and its application to aviation and space. materials of SAMPE, 326-335.

[42] Shrestha, S., Wang, B., & Dutta, P. (2020). Nanoparticle processing: Understanding and controlling aggregation. Advances in colloid and interface science, 279, 102162.

[43] Liu, S., Reed, S. N., Higgins, M. J., Titus, M. S., & Kramer-Bottiglio, R. (2019). Oxide rupture-induced conductivity in liquid metal nanoparticles by laser and thermal sintering. Nanoscale, 11(38), 17615-17629.